

# NUMERICAL STUDY ON THE INTERACTION BETWEEN PERIODIC WAVES AND AN FLEXIBLE WALL

Zhengyu Hu, National University of Singapore, [z.hu@u.nus.edu](mailto:z.hu@u.nus.edu)  
 Yuzhu Li, National University of Singapore, [pearl.li@nus.edu.sg](mailto:pearl.li@nus.edu.sg)

## INTRODUCTION

Coastal structures were usually considered as stiff in the majority of studies related to wave-structure interaction. In certain situations, such as impulsive wave loading on flexible breakwaters, ship hulls, tank walls, hydroelasticity can be of importance for both wave dynamics and structural responses. Akriş et al. (2018) showed that hydroelastic effects can either relax or amplify the hydrodynamic characteristics (i.e., wave run-up and force) and structural oscillations in a deformable cantilever wall interacting with an incident wave group. For flexible coastal defenses, Huang and Li (2022) showed that an elastic horizontal plate breakwater can exhibit a better performance of wave damping than a rigid one. Sree et al. (2021) experimentally investigated a submerged horizontal viscoelastic plate under surface waves. They reported a complete cutoff of the wave energy with the flexible plate. However, the hydroelasticity of a steep-fronted structure in nonlinear progressive waves was not yet studied in a detailed manner, which requires advanced numerical methods for modelling the nonlinear interaction between the fluid and the solid with finite deformations.

The present study focuses on the hydroelastic behavior of a flexible vertical wall in nonlinear periodic waves with different wave periods (or frequencies). The effects of the structural stiffness on the wave evolution and the structural deformation are investigated with a fully-coupled wave-structure interaction model.

## FULLY-COUPLED NUMERICAL MODEL

The present numerical model fully coupled the computational fluid dynamics (CFD) and computational solid mechanics (CSM) models. A partitioned scheme is used for the CFD+CSM coupling. It enforces the momentum and kinematic continuity at the fluid-solid interface with a Dirichlet-Neumann approach (Cardiff et al., 2018; Tuković et al., 2018).

The CFD model solves the Navier-Stokes equations for the multi-phase incompressible, isothermal, and Newtonian flow with a free surface (i.e., interface between air and water). The free surface is captured by the Volume of Fluid (VOF) approach (Hirt and Nichols, 1981). The wave generation combined with an active absorption is initialized by IHFOAM in the framework of OpenFOAM (Higuera et al., 2013), in which waves are generated using a stream function theory (Fenton, 1985). The laminar flow model is assumed in the present simulation since the turbulence effects are expected to be negligible in non-breaking waves. The CSM model calculates the Cauchy stress tensor with the nonlinear Neo-Hookean hyperelastic law. The integration of the momentum equation in the total Lagrangian form (refer to the initial undeformed configuration). A number of fluid-structure interaction iterations are required per time step.

## MODEL SETUP AND VERIFICATION

Figure 1 shows a sketch of the numerical flume with a fixed water depth ( $h$ ) in the Cartesian coordinate system. Waves are generated at the wave inlet boundary. A flexible cantilever wall (bottom fixed and top free) is clamped at the center ( $O$ ) of the wave flume. For the applicability of analysis, the mass coefficient ( $\gamma = \rho_s b / \rho_w h$ ) and the stiffness coefficient ( $\beta = EI / \rho_w g h^4$ ) are used to represent the mechanical properties of the wall, where  $\rho_s$  and  $\rho_w$  are the densities of the wall and the water,  $b$  is the thickness,  $E$  is Young's modulus,  $I$  is the moment of inertia, and  $g$  is the gravity acceleration. The radiated waves stimulated by the wall's deformation are absorbed in the wave outlet boundary. The top and bottom of the numerical flume are specified as atmospheric and no-slip boundary conditions, respectively. The interfaces of the wall with the fluid are set as the Dirichlet-Neumann boundary conditions (Cardiff et al., 2018).

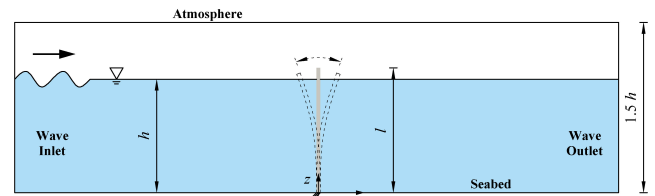


Figure 1 - Sketch of the numerical flume (not to scale)

The present model is verified against the numerical results of He and Kashiwagi (2012), who studied the hydroelastic behavior of a cantilever wall interaction with a solitary wave. A solitary wave with a wave height ( $H$ ) of  $0.04h$  is generated  $50h$  from the wall. The mass coefficient  $\gamma$  and the stiffness coefficient  $\beta$  of the wall are 0.01 and 0.04, respectively. The length of the wall is  $1.1h$ . The computational mesh utilized in the fluid domain is 15 cells/ $H$  with the aspect ratio of 1/3 and that in the solid domain is 600 cells (i.e.,  $6 \times 100$  cells).

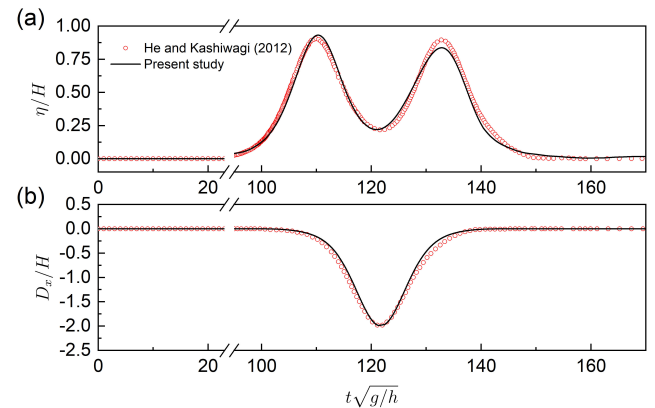


Figure 2 - Comparison of the results between the present study and He and Kashiwagi (2012)

Figure 2 shows the comparisons of the wave elevation at  $x = -10h$  and the horizontal displacement of the wall at  $z = h/2$  between the present study and He and Kashiwagi (2012). Good agreement is obtained in both the wave evolution and the structural displacement. Therefore, this model setup and mesh configuration is used in the following simulations. The present study focuses on periodic waves interactions with a flexible vertical wall. For the periodic waves, the wave height is  $0.1h$  and the wave period ( $T$ ) ranges from 1.0 to 1.6 s in an interval of 0.1 s, where  $h = 0.3$  m. For the wall, the mass coefficient  $\gamma$  is 0.06, the stiffness coefficient  $\beta$  ranges from 0.08 to 0.20 in an interval of 0.04, and the length is  $1.1h$ .

### HYDROELASTIC BEHAVIORS OF THE WALL

Figure 3 shows the comparison of the reflection coefficient  $C_r$  (i.e., the ratio of the reflected wave height to the incident wave height) and the transmission coefficient  $C_t$  (i.e., the ratio of the radiated wave height to the incident wave height) induced by the flexible wall with different stiffness. It is observed that  $C_r$  increases with the increasing wave period. This increase is more obvious for the most elastic wall. Besides,  $C_r$  also increases with the increasing structural stiffness, which is more sensitive for waves with a relatively larger wave period. Note that the values of  $C_r^2 + C_t^2$  are close to 1 with negligible wave dissipation. Therefore, the tendencies of  $C_t$  against  $T$  and  $\beta$  are in contrast with  $C_r$ .

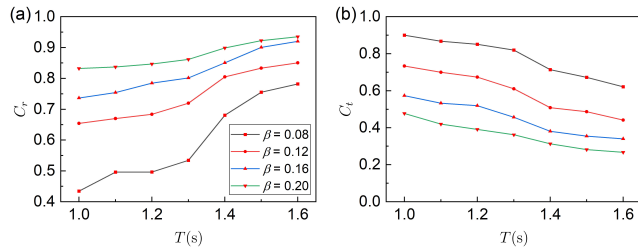


Figure 3 - Reflection and transmission coefficients

Figure 4 shows the deformation of the wall with  $\beta = 0.08$  in periodic waves with the wave period  $T$  of 1.2 s. In Figure 4a, the maximum offshore horizontal displacement ( $D_{min}$ ) of the wall occurs at  $0.6T$  instead of at the wave trough (i.e.,  $0.5T$ ). This implies a  $0.1T$  phase lag between the wall's displacement and the wave surface elevation. The maximum von-Mises stress ( $\sigma_v/\rho_w g h$ ) is distributed near the fixed end. It gradually decreases to zero from the bottom to the free end. In Figure 4b, as the wave propagates, the maximum shoreward horizontal displacement ( $D_{max}$ ) occurs at  $1.1T$ . Both the magnitudes of  $D$  and  $\sigma_v/\rho_w g h$  are slightly larger than that at  $0.6T$ , because the fluid in the wave crest moves faster than that in the wave trough due to wave asymmetry. Wave overtopping is not observed herein.

### CONCLUSIONS

The present work numerically studied the interaction between periodic waves and a flexible wall. The reflection coefficient increases with the wave period and the wall stiffness, in contrast to the transmission coefficient. The wall's displacement presents a slight phase lag relative to the wave elevation. Both the displacement and the stress of the wall tend to be larger in the shoreward direction than the offshore direction, because of the asymmetry of wave crests

and troughs. The present study also showed that wave overtopping can be mitigated with an elastic wall due to the decrease in the reflection coefficient.

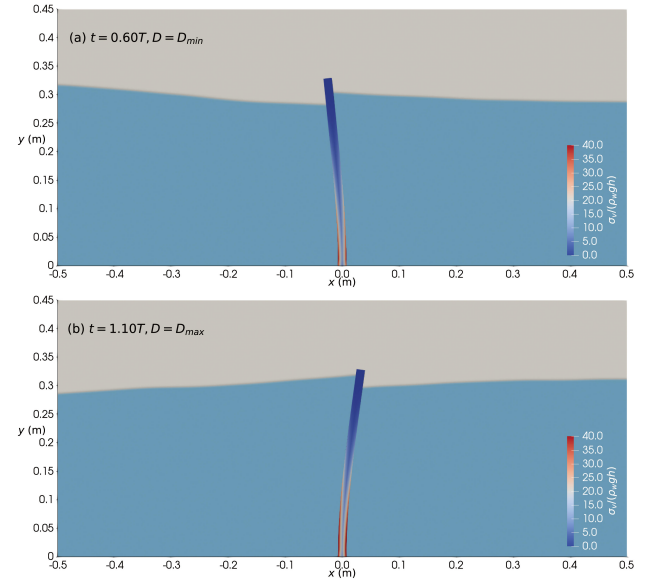


Figure 4 - Snapshots of the wall deformation in periodic waves

### REFERENCES

- Akrish, G., Rabinovitch, O. and Agnon, Y. (2018): Hydroelasticity and nonlinearity in the interaction between water waves and an elastic wall. *Journal of Fluid Mechanics*, vol. 845, pp. 293-320.
- Cardiff, P. et al. (2018): An open-source finite volume toolbox for solid mechanics and fluid-solid interaction simulations. arXiv preprint arXiv:1808.10736.
- Fenton, J.D. (1985): A fifth-order stokes theory for steady waves. *Journal of Waterway, Port, Coastal, and Ocean Engineering*, vol. 111, pp. 216-234.
- He, G. and Kashiwagi, M. (2012): Numerical analysis of the hydroelastic behavior of a vertical plate due to solitary waves. *Journal of Marine Science and Technology*, vol. 17, pp. 154-167.
- Higuera, P., Lara, J.L. and Losada, I.J. (2013): Realistic wave generation and active wave absorption for navier-stokes models: Application to openfoam®. *Coastal Engineering*, vol. 71, pp. 102-118.
- Hirt, C.W. and Nichols, B.D. (1981): Volume of fluid (vof) method for the dynamics of free boundaries. *Journal of Computational Physics*, vol. 39, pp. 201-225.
- Huang, L. and Li, Y. (2022): Design of the submerged horizontal plate breakwater using a fully coupled hydroelastic approach. *Computer-Aided Civil and Infrastructure Engineering*, vol. 37, pp. 915-932.
- Sree, D.K.K., Mandal, S. and Law, A.W.-K. (2021): Surface wave interactions with submerged horizontal viscoelastic sheets. *Applied Ocean Research*, vol. 107.
- Tuković, Ž., Karač, A., Cardiff, P., Jasak, H. and Ivanković, A. (2018): Openfoam finite volume solver for fluid-solid interaction. *Transactions of FAMENA*, vol. 42, pp. 1-31.